

## Supporting Information

### Acceptor Aggregation Induced Hole Mobility Degradation in Polymer Solar Cells

Yiyun Li,<sup>1</sup> Dongcheng Jiang,<sup>1</sup> Jiangkai Sun,<sup>1</sup> Rui Shi,<sup>1</sup> Yu Chen<sup>3</sup>, Mingsheng Xu<sup>2</sup>,  
Xiaoyan Du,<sup>1</sup> Guofu Xu,<sup>1\*</sup>, Hang Yin<sup>1\*</sup>

#### Affiliations:

<sup>1</sup> School of Physics, State Key Laboratory of Crystal Materials, Shandong University,  
Jinan, 250100, China.

<sup>2</sup> School of Integrated Circuits, Shandong University, Jinan, 250100, China.

<sup>3</sup> Beijing Synchrotron Radiation Facility, Institute of High Energy Physics, Chinese  
Academy of Sciences, Beijing, 100049, China

\* Corresponding author: Guofu Xu, [xgf@sdu.edu.cn](mailto:xgf@sdu.edu.cn); Hang Yin, [hyin@sdu.edu.cn](mailto:hyin@sdu.edu.cn)

Keywords: Organic semiconductors, Charge carrier transport, Device stability, Organic solar cells

**Device Fabrication:** OPV devices with the structure of ITO/PEDOT:PSS/Active-layer/ PNDIT-F3N-Br/Ag were fabricated. Patterned ITO substrates were cleaned in sequence in detergent, deionized water, acetone, and isopropanol in an ultrasonic bath for 20 min respectively. Then the ITO substrates were treated with ultraviolet-ozone for 15 min. PEDOT:PSS solution (PEDOT:PSS:deionized water is 1:1) was spin-coated onto the ultraviolet ozone-treated ITO substrates, followed by annealing at 150 °C for 20 min in the ambient conditions. The PM6:Y6 photoactive blend solution is dissolved in chloroform:1-chloronaphthalene (99.5:0.5 vol%) solvent. Similarly, the PM6:PY-IT photoactive blend solution is dissolved in chloroform:1-chloronaphthalene (97:3 vol%) solvent. Both solutions are stirred at 45°C for 2 hours. The PM6:Y6 blend solution is spin-coated onto the top of the PEDOT:PSS layer at 3000 rpm for 30 seconds, while

the PM6:PY-IT blend solution is spun at 2500 rpm. Subsequently, both solutions are annealed at 100°C for 10 minutes in the N<sub>2</sub> glovebox. Then the PNDIT-F3N-Br solution (0.5 mg mL<sup>-1</sup> in methanol) was spin-coated onto the active layer at 3000 rpm for 30 s, followed by thermal deposition of Ag (100 nm) top electrode under high vacuum ( $< 2.5 \times 10^{-4}$  Pa) to fabricate devices. Hole-only devices with ITO/PEDOT:PSS/Active-layer/Spiro-TPD/Au and electron-only devices with ITO/Al/Active-layer/PDINN/Ag structure were fabricated similarly.

**Aging conditions:** The devices are encapsulated and placed in darkness on a constant temperature heating plate at 60 degrees Celsius for aging.

**Grazing Incidence Wide-Angle X-ray Scattering (GIWAXS) Measurement:**

GIWAXS measurements were performed upon a film-depth dependent light absorption spectrometer Xeuss 2.0 (Xenocs Inc.) under vacuum conditions. X-rays have a wavelength of 1.54189 Å and sample detector distance calibrated by a silver behenate. Samples were prepared on silicon substrates using identical blend solutions as those used in devices. The thermal aging conditions of the films are the same as the OSCs.

**AFM and PiFM Measurement:** Samples were prepared on gold substrates using the same blend solution as that used in the devices. The thermal aging conditions of the samples were identical to those of the OSCs.

**Film-depth-dependent Light Absorption Spectroscopy (FLAS).**

FLAS measurements were performed using a film-depth-dependent light absorption spectrometer (PU100, Puguangweishi Co. Ltd). In-situ soft plasma etching at low pressure (less than 20 Pa) was utilized to extract the depth-resolved absorption spectrum for the organic active layer. Beer-Lambert's law was applied to fit the FLAS results, which were subsequently used to fit the exciton generation contour using a modified optical matrix-transfer approach.

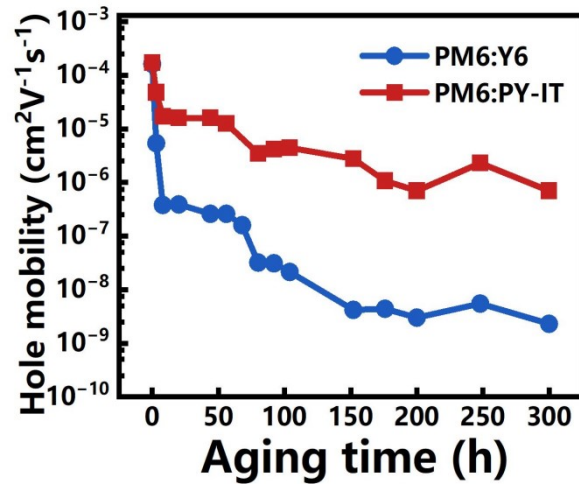


**Figure S1.** Hole mobility as a function of thermal aging time. (D:A = 1:1.2).

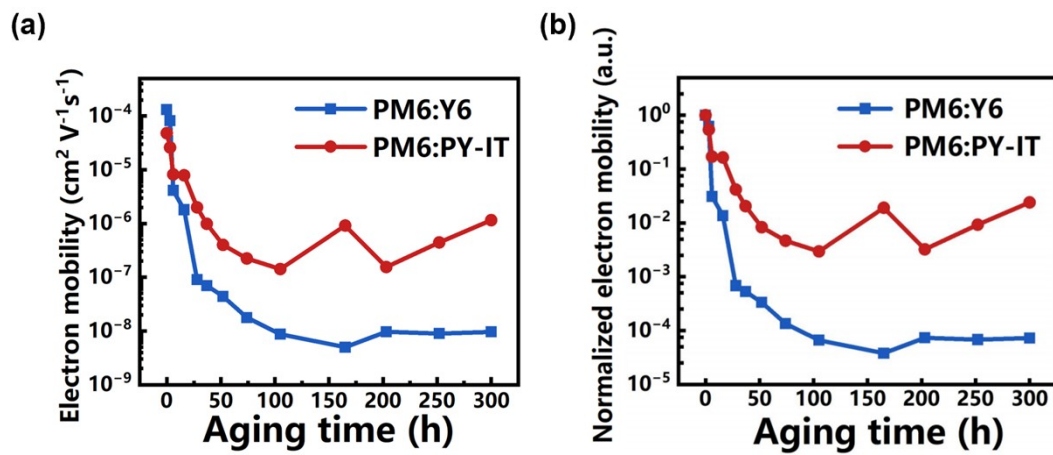


**Figure S2.** Electron mobility as a function of thermal aging time. (D:A = 1:1.2)

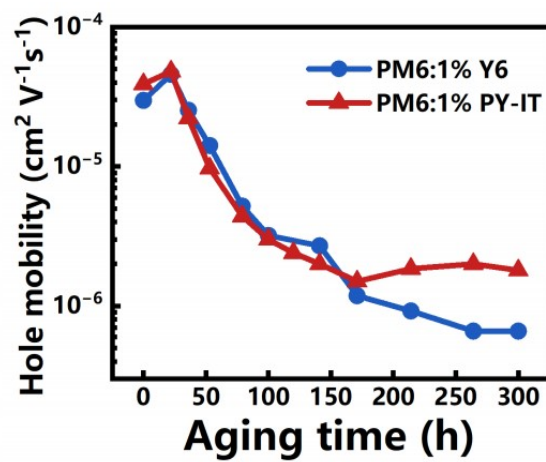


**Figure S3.** Hole mobility as a function of thermal aging time. (D:A = 99:1)

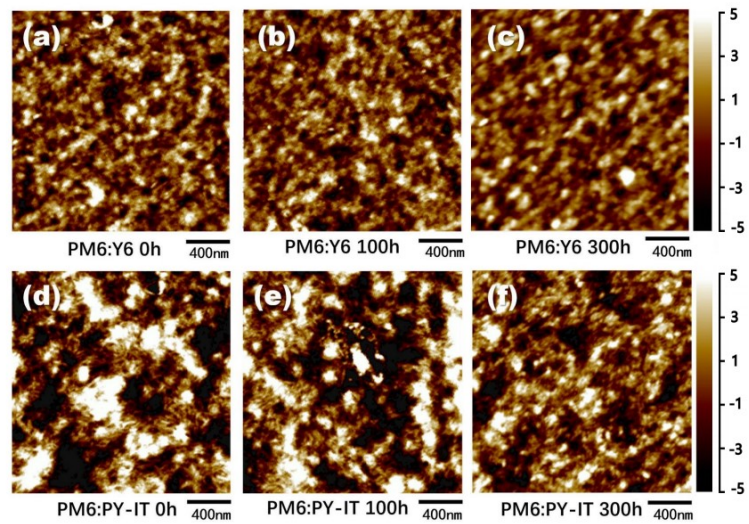


**Figure S4.** AFM images of the two systems blended film before and after thermal aging.

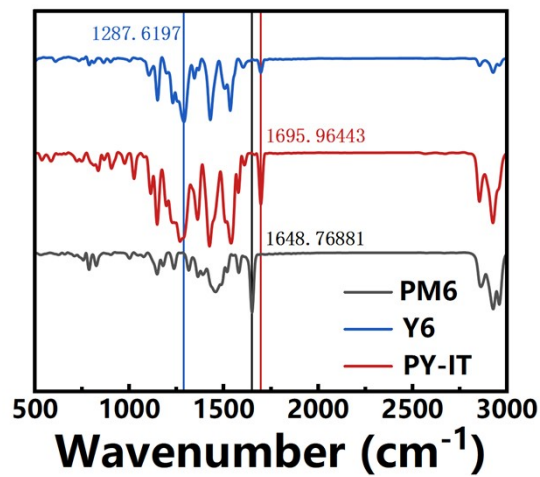


**Figure S5.** Fourier infrared spectra and characteristic peaks of the three materials.

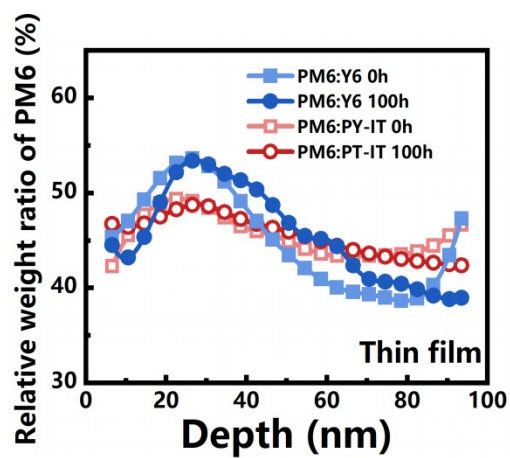


**Figure S6.** Evolution of vertical phase distribution of PM6:Y6 and PM6:PY-IT thin films before and after thermal aging.

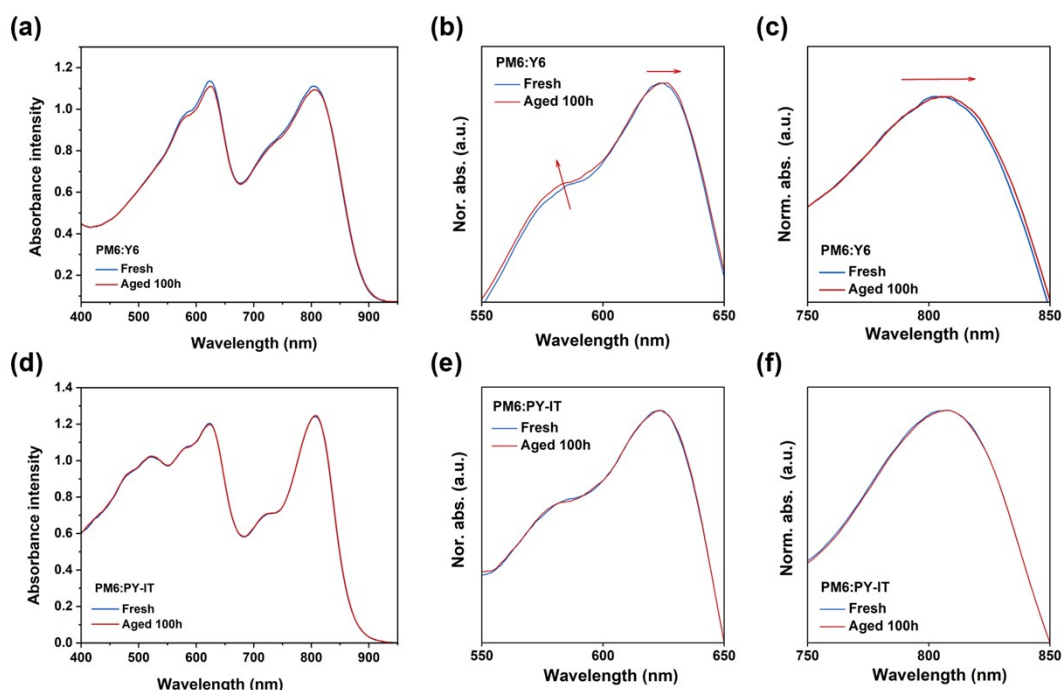


**Figure S7.** (a) UV-Vis absorption spectra of the PM6:Y6 blend film in fresh and aged states. (b) Absorption spectra of the PM6 component in the PM6:Y6 system. (c) Absorption spectra of the Y6 component in the PM6:Y6 system. (d) UV-Vis absorption spectra of the PM6:PY-IT blend film in fresh and aged states. (e) Absorption spectra of the PM6 component in the PM6:PY-IT system. (f) Absorption spectra of the Y6 component in the PM6:PY-IT system.

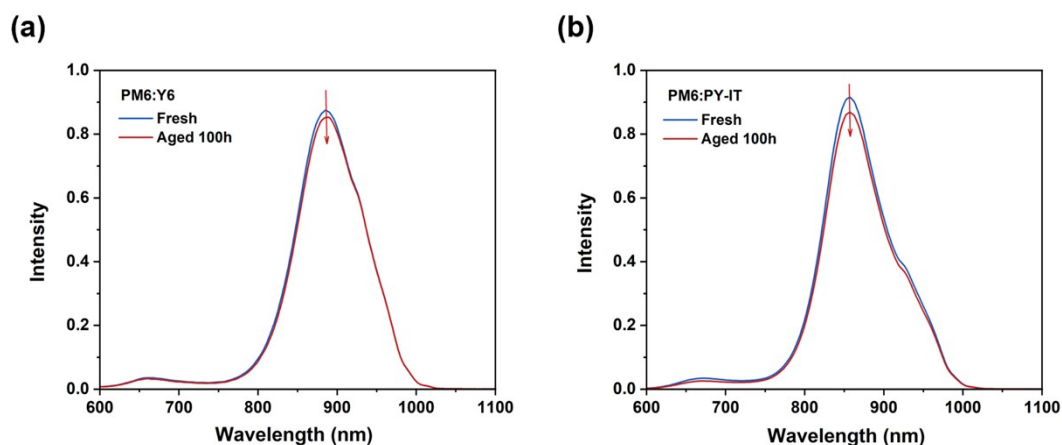


**Figure S8.** (a) PL spectra of the PM6:Y6 system in fresh and aged states. (b) PL spectra of the PM6:PY-IT system in fresh and aged states.

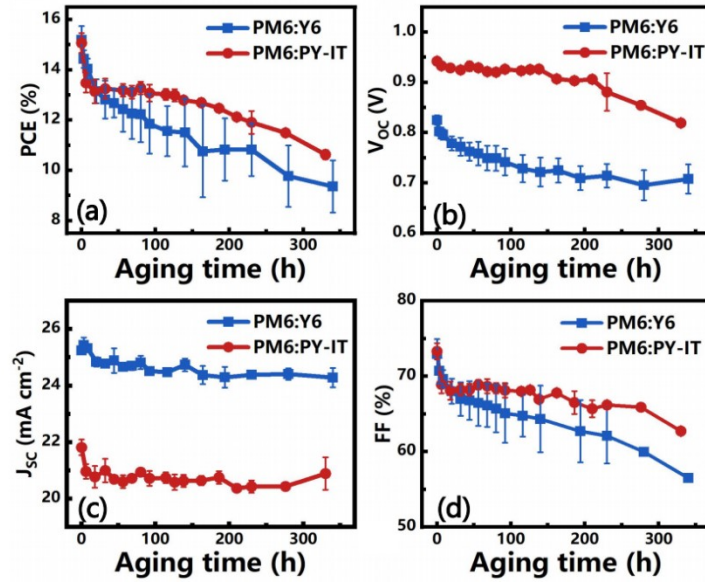


**Figure S9.** Trend of raw values of device parameters during thermal aging. (a). PCE (b).  $V_{OC}$  (c).  $J_{SC}$  (d). FF

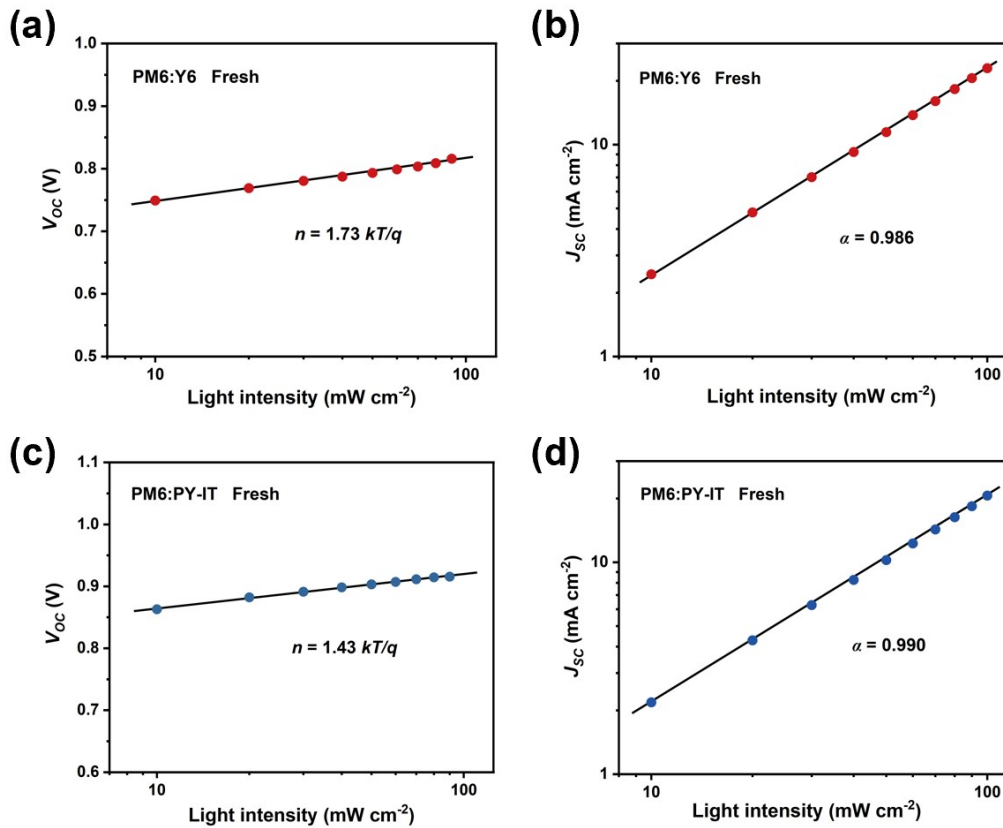


**Figure S10.** Light intensity dependence of  $V_{OC}$  and  $J_{SC}$ : (a), (b) PM6:Y6; (c), (d) PM6:PY-IT.